Supplementary Materials:

An MdsABC-Mediated Pathway for Pathogenicity in *Salmonella* Typhimurium

Saemee Song[1,3], Boeun Lee[1], Ji-Hyun Yeom[1], Soonhye Hwang[1], Ilnam Kang[2], Jang-Cheon Cho[2], Nam-Chul Ha[3], Jeehyeon Bae[4], Kangseok Lee[1*], and Yong-Hak Kim[5*]

[1]Department of Life Science, Chung-Ang University, Seoul, Republic of Korea

[2]Department of Biological Sciences, Inha University, Incheon, Republic of Korea

[3]Department of Food and Animal Biotechnology, Department of Agricultural Biotechnology, Seoul National University, Seoul, Republic of Korea

[4]College of Pharmacy, Chung-Ang University, Seoul, Republic of Korea

[5]Department of Microbiology, Catholic University of Daegu School of Medicine, Daegu, Republic of Korea.

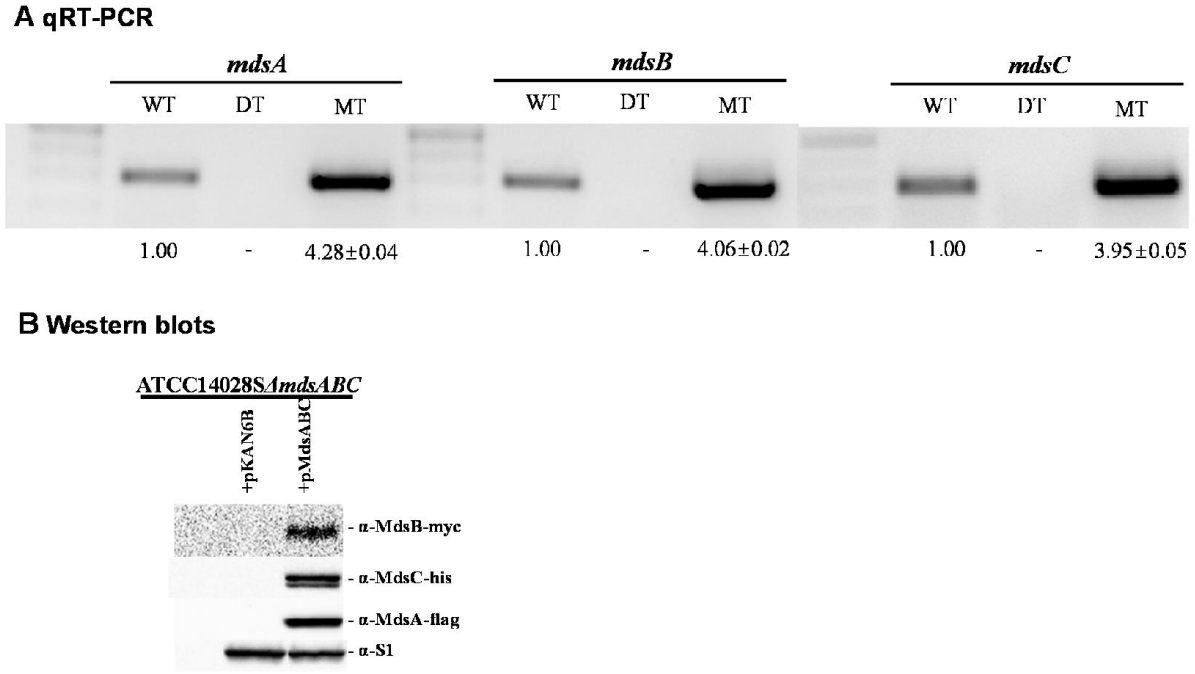

FIG S1 Arabinose-induced expression levels of the *mdsABC* genes in the MdsABC expression mutant (MT) strain of *Salmonella enterica* Typhimurium 14028S. (A) Results from reverse-transcriptase and polymerase chain reaction (RT-PCR) for the determination of relative expression (mRNA) levels of *mdsABC* gene transcripts in the RNA extracts of wild-type (WT), *mdsABC* deletion (DT), and *mdsABC* expression mutant (MT) strains of *S.* Typhimurium 14028S cultivated with LB medium containing 0.1% arabinose. Relative levels of *mdsABC* expression in the MT strain were calculated after normalization to the corresponding gene expression levels in the WT strain. Results from three independent samples are reported as means ± standard deviations. Dashes, not detected. (B) Western blot analysis of MdsABC proteins expressed with flag, *c*-myc, and hexahistidine tags in the MT strain containing the pMdsABC expression vector, but not expressed in the WT strain containing the empty pKAN6B plasmid. The RpsA (S1) protein was detected as a housekeeping protein to compare the protein expression levels. The western blot analysis was performed with appropriate antibodies, as described in the previous study (Song *et al.*, 2014).

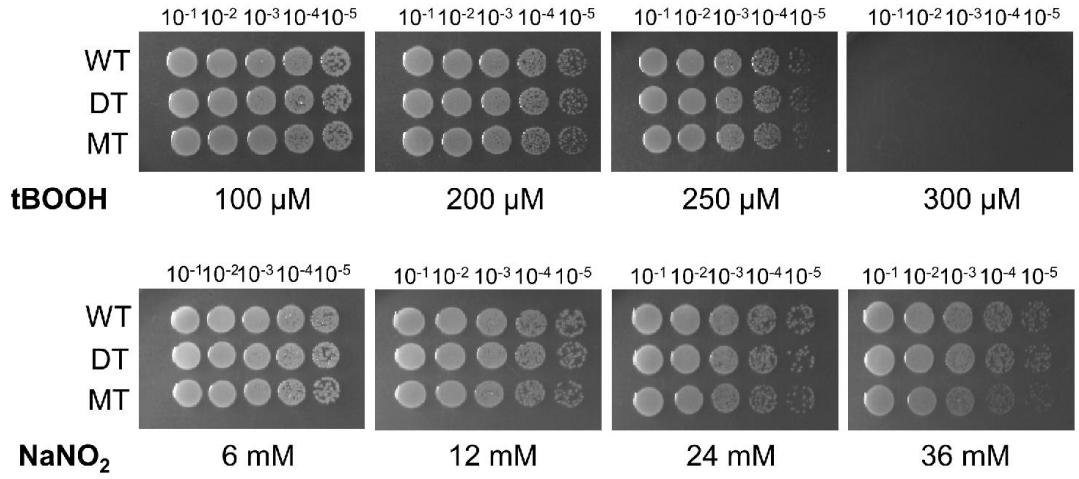

FIG S2 Effects of MdsABC on resistance to t-BOOH and $NaNO_2$. Spot dilution assays of the wild-type (WT), *mdsABC* deletion (DT), and *mdsABC* expression mutant (MT) strains of *S.* Typhimurium 14028S on LB agar plates containing appropriate concentrations of t-BOOH, and $NaNO_2$. Colony growth was observed after 12-18 h of incubation at 37°C. Overexpression of MdsABC had no effect on bacterial resistance to t-BOOH and $NaNO_2$.

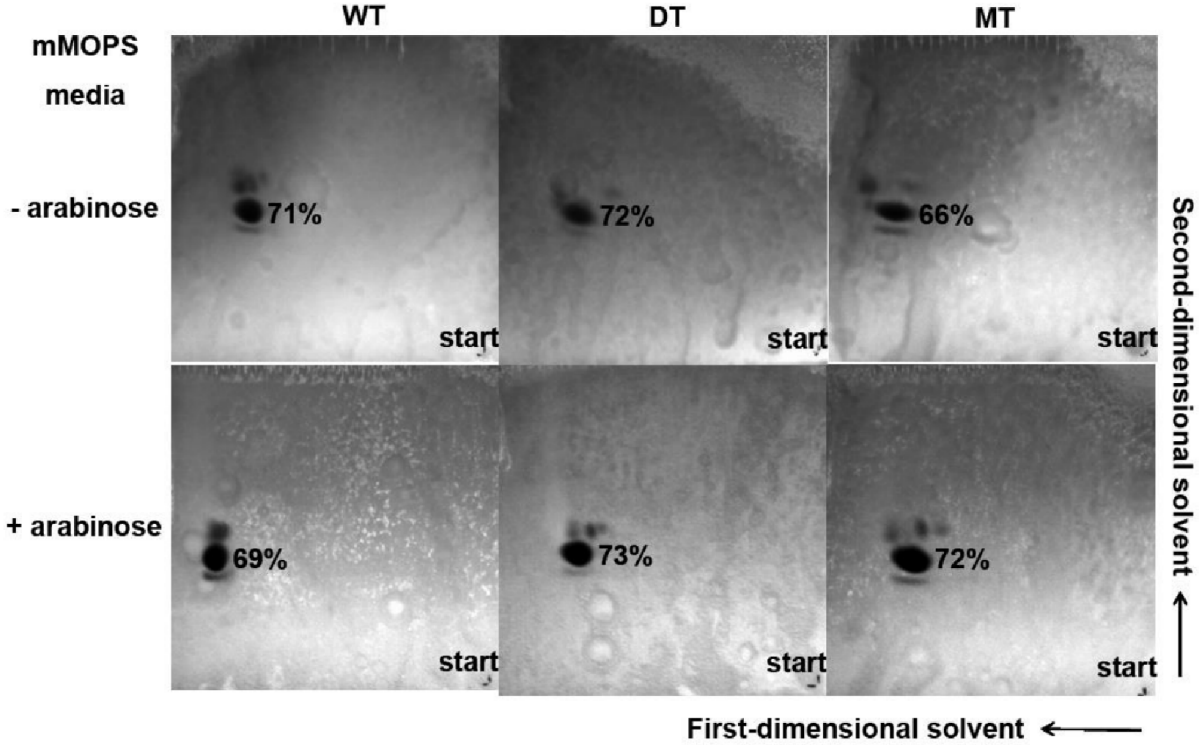

FIG S3 Two-dimensional TLC analysis of cellular phospholipids. Phospholipids were extracted from the WT (wild-type), DT (*ΔmdsABC*), and MT (pMdsABC) strains of *Salmonella* Typhimurium 14028S cultivated in mMOPS media in the presence or absence of 0.1% arabinose. Two-dimensional TLC of the cellular lipids was conducted using chloroform-methanol-water-28% aqueous ammonia (130:70:8:0.5 by volume) in the first dimension followed by chloroform-acetone-methanol-acetic acid-water (100:40:20:20:10 by volume) in the second. Phospholipid spots were visualized by molybdenum blue staining solution spray, and the percentage of PL-1 compound area, analyzed using ImageQuant software (GE Healthcare Life Sciences), is shown in each silica gel.

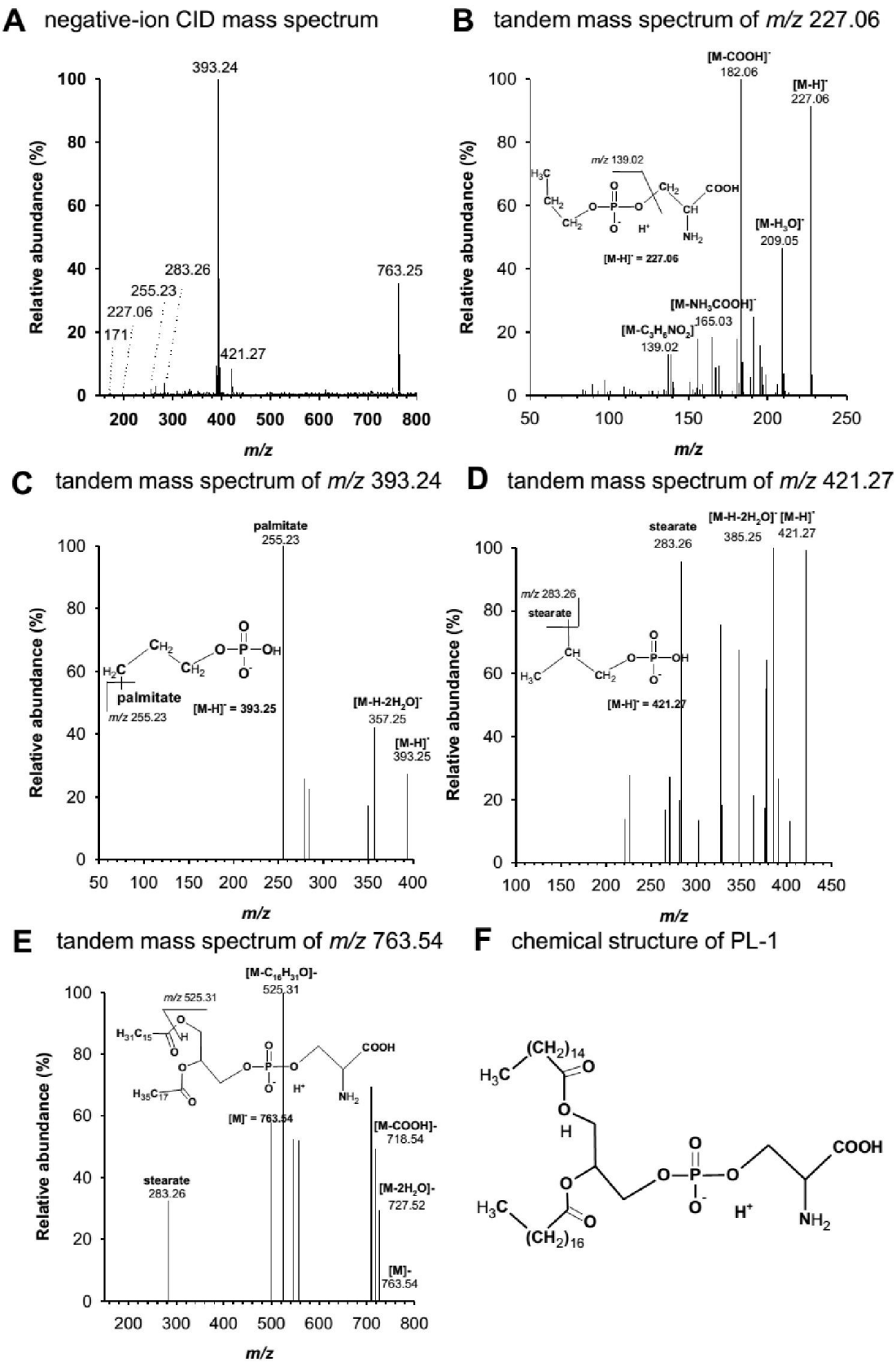
A negative-ion CID mass spectrum
393.24
283.26
255.23
227.06
171
421.27
763.25
Relative abundance (%)
m/z
B tandem mass spectrum of m/z 227.06
[M-COOH]⁻
182.06
[M-H]⁻
227.06
m/z 139.02
[M-H]⁻ = 227.06
[M-H₂O]⁻
209.05
[M-NH₃COOH]⁻
165.03
[M-C₃H₆NO₂]⁻
139.02
C tandem mass spectrum of m/z 393.24
palmitate
255.23
[M-H]⁻ = 393.25
[M-H-2H₂O]⁻
357.25
[M-H]⁻
393.25
D tandem mass spectrum of m/z 421.27
stearate
283.26
[M-H-2H₂O]⁻
385.25
[M-H]⁻
421.27
m/z 283.26
[M-H]⁻ = 421.27
E tandem mass spectrum of m/z 763.54
[M-C₁₆H₃₁O]-
525.31
m/z 525.31
[M]⁻ = 763.54
[M-COOH]-
718.54
[M-2H₂O]-
727.52
[M]-
763.54
stearate
283.26
F chemical structure of PL-1
COOH
NH₂
H⁺

FIG S4 Mass analysis of purified PL-1 hypersecreted from *mdsABC*-overexpressing mutant (MT) bacteria of *Salmonella* Typhimurium 14028S. (A) Electrospray and collision-induced fragmentation of PL-1 in the negative-ion mode. (B) Tandem mass spectrum of the *m/z* 277.06 ion, assigned to the CID fragments of propyl phosphoserine. (C) Tandem mass spectrum of the *m/z* 393.24 ion, assigned to the CID fragments of 1-palmitoyl-2-deoxyglycero-3-phosphate. (D) Tandem mass spectrum of the *m/z* 421.27 ion, assigned to the CID fragments of 2-stearoyl-1-deoxyglycero-3-phosphate. (E) Tandem mass spectrum of the *m/z* 763.54 ion, assigned to the molecular ion and fragment ions generated from 1-palmitoyl-2-stearoyl-*sn*-glycero-3-phosphoserine (phosphatidylserine). (F) Proposed chemical structure of 1-palmitoyl-2-stearoyl-phosphatidylserine (PSPS) identified by ESI/CID mass spectrometry in negative-ion mode.

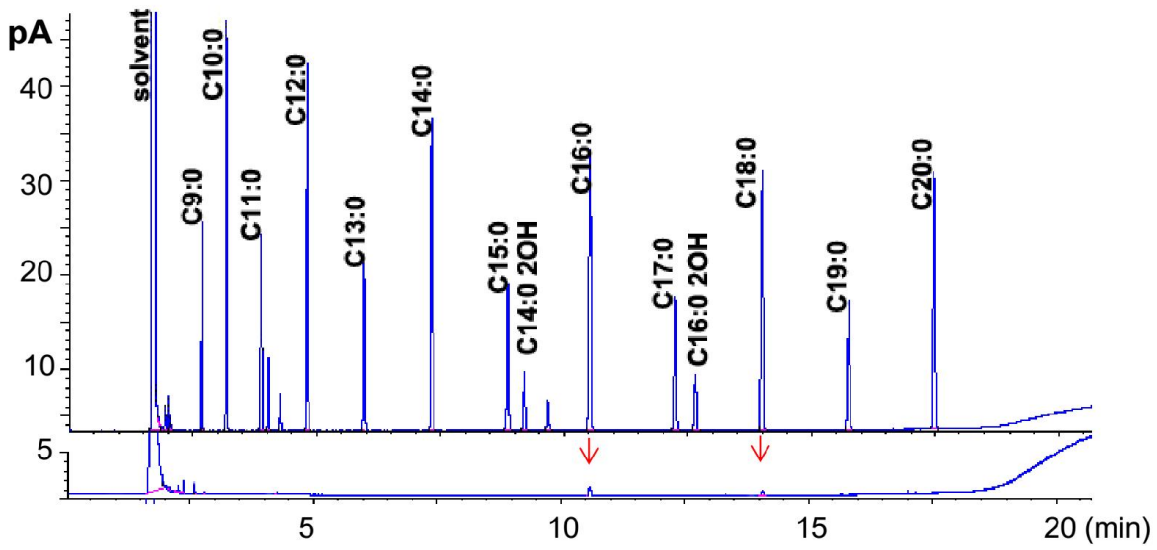

FIG S5 Gas chromatograms of fatty acid methyl ester MIDI standards (upper) and methyl esters derived from purified PL-1 compound (bottom). The two peaks derived from the PL-1 sample, which eluted at 10.52 and 14.01 min, correspond to palmitate (C16:0) and stearate (C18:0) methyl esters, respectively, as indicated by arrows.

FIG S6(A-K) Tandem mass spectra and assigned *b*- and *y*-ions of reactive cysteine-containing peptides of membrane-bound proteins. Proteins have the potential to form intermolecular disulfide bonds via diamide-mediated *S*-thiolation, as shown in Fig. 5A in the main text. To distinguish between free cysteine and DTT reduced cysteine thiol groups, free cysteine residues of proteins were blocked with *N*-ethylmaleimide prior to iodoacetamide modification (carbamidomethylation) of DTT reduced cysteine residues..

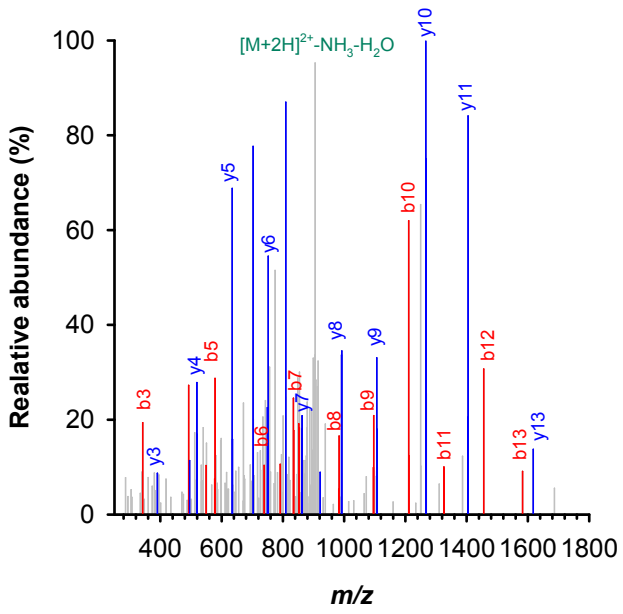

Assigned *b*- and *y*-ions

#	b+	b++	Seq.	y+	y++	#
1			L	1843.81	922.41	15
2	227.18		I	1730.73	865.87	14
3	342.2	171.61	D	1617.64	809.33	13
4	441.27	221.14	V	1502.62	751.81	12
5	578.33	289.67	H	1403.55	702.28	11
6	738.36	369.68	C#	1266.49	633.75	10
7	853.39	427.2	D	1106.46	553.73	9
8	982.43	491.72	E	991.43	496.22	8
9	1095.51	548.26	I	862.39	431.7	7
10	1210.54	605.77	D	749.31	375.16	6
11	1325.57	663.29	D	634.28	317.64	5
12	1454.61	727.81	E	519.25	260.13	4
13	1582.67	791.84	Q	390.21	195.61	3
14	1669.7	835.35	S	262.15		2
15			R	175.12		1

Sequest results: *z*= +2, *m/z* = 922.72 (mass error: -278.26 ppm), Xcorr = 3.48, SpScore = 1029.82

FIG S6(A) Assignment of the tandem mass spectrum to predicted *b*- and *y*-ions of cysteine deaminase (CodA) ^{210}LIDVHC#DEIDDEQSR^{224}, which forms an intermolecular disulfide bond at Cys215.

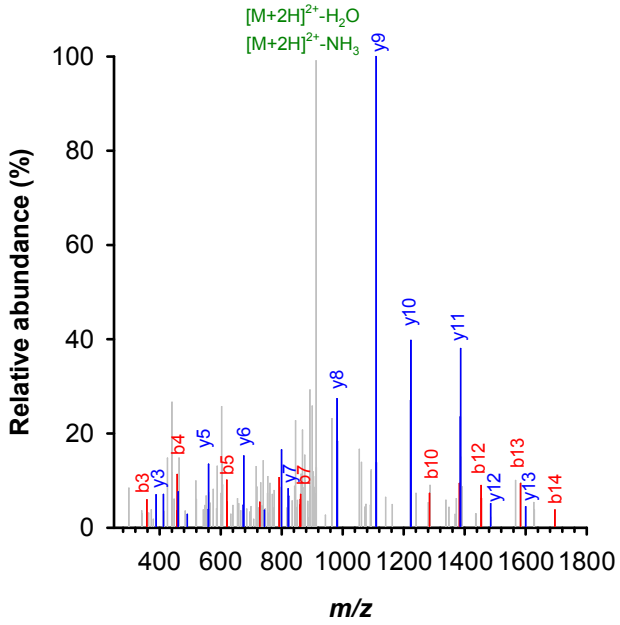

Assigned *b*- and *y*-ions

#	b+	b++	Seq.	y+	y++	#
1			Q	1841.87	921.44	15
2	244.09		D	1713.81	857.41	14
3	**358.14**	179.57	N	**1598.79**	**799.9**	13
4	**457.2**	229.11	V	**1484.74**	**742.88**	12
5	**620.27**	310.64	Y	**1385.68**	693.34	11
6	733.35	367.18	L	**1222.61**	611.81	10
7	**861.41**	431.21	Q	**1109.53**	555.27	9
8	1021.44	511.22	C#	**981.47**	**491.24**	8
9	1168.51	584.76	F	**821.44**	**411.22**	7
10	**1283.54**	642.27	D	**674.37**	337.69	6
11	**1382.61**	691.81	V	**559.34**	280.18	5
12	**1453.64**	**727.32**	A	**460.28**	230.64	4
13	**1582.68**	**791.85**	E	**389.24**	195.12	3
14	**1695.77**	848.39	L	260.2		2
15			K	147.11		1

Sequest results: *z*= +2, *m/z* = 921.97 (mass error: -68.95 ppm), Xcorr = 3.21, SpScore = 1174.74

FIG S6(B) Assignment of the tandem mass spectrum to predicted *b*- and *y*-ions of glycerophosphodiester phosphodiesterase (GlpQ) ^{199}QDNVYLQC#FDVAELK^{213}, which forms an intermolecular disulfide bond at Cys206.

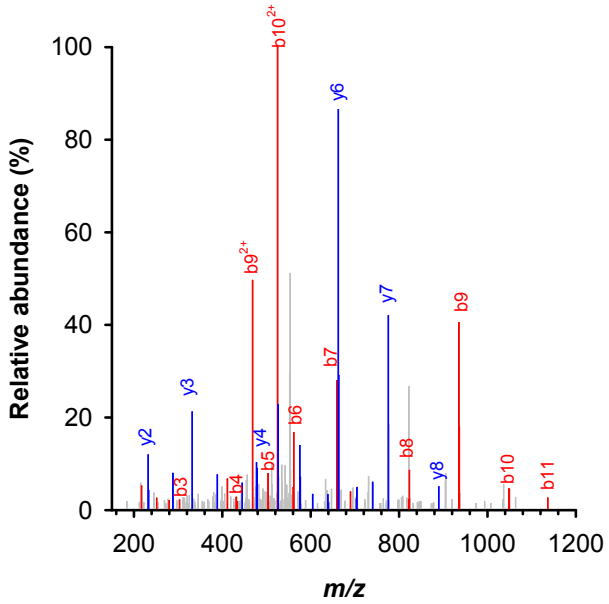

Assigned *b*- and *y*-ions

#	b	b++	Seq.	y	y++	#
1			A	1709.87	855.44	16
2	**232.08**		C#	1638.83	819.92	15
3	**303.11**	152.06	A	1478.8	**739.9**	14
4	**432.16**	**216.58**	E	1407.76	**704.38**	13
5	**503.19**	**252.1**	A	1278.72	**639.86**	12
6	**560.21**	**280.61**	G	1207.68	**604.35**	11
7	**659.28**	330.14	V	1150.66	**575.83**	10
8	**822.35**	**411.68**	Y	1051.59	**526.3**	9
9	**935.43**	**468.22**	L	**888.53**	**444.77**	8
10	**1048.51**	**524.76**	I	**775.45**	**388.23**	7
11	**1135.55**	568.28	S	**662.36**	**331.68**	6
12	1232.6	616.8	P	**575.33**	**288.17**	5
13	1379.67	**690.34**	F	**478.28**	239.64	4
14	1478.74	**739.87**	V	**331.21**	166.11	3
15	1535.76	768.38	G	**232.14**		2
16			R	175.12		1

Sequest results: *z*= +3, *m/z* = 570.89 (mass error: -201.88 ppm), Xcorr = 3.55, SpScore = 1412.76

FIG S6(C) Assignment of the tandem mass spectrum to predicted *b*- and *y*-ions of transaldolase B (TalB) ^{166}AC#AEAGVYLISPFVGR^{181}, which forms an intermolecular disulfide bond at Cys167.

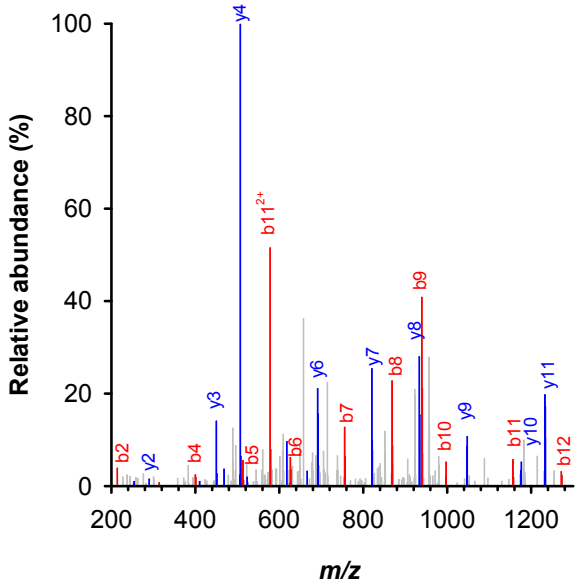

Assigned *b*- and *y*-ions

#	b	b++	Seq.	y	y++	#
1			N	1445.71	723.36	13
2	214.12		V	1331.66	666.33	12
3	271.14		G	1232.59	616.8	11
4	400.18	200.6	E	1175.57	588.29	10
5	513.27	257.14	I	1046.53	523.77	9
6	626.35	313.68	L	933.45	467.23	8
7	755.39	378.2	E	820.36	410.68	7
8	868.48	434.74	L	691.32	346.16	6
9	939.52	470.26	A	578.23	289.62	5
10	996.54	498.77	G	507.2	254.1	4
11	1156.57	578.79	C#	450.18	225.59	3
12	1271.59	636.3	D	290.15		2
13			R	175.12		1

Sequest results: *z*= +2, *m/z* = 723.74 (mass error: -111.11 ppm), Xcorr = 3.89, SpScore = 1551.42

FIG S6(D) Assignment of the tandem mass spectrum to the predicted *b*- and *y*-ions of transaldolase B (TalB) ^{229}NVGEILELAGC#DR^{241}, which forms an intermolecular disulfide bond at Cys239.

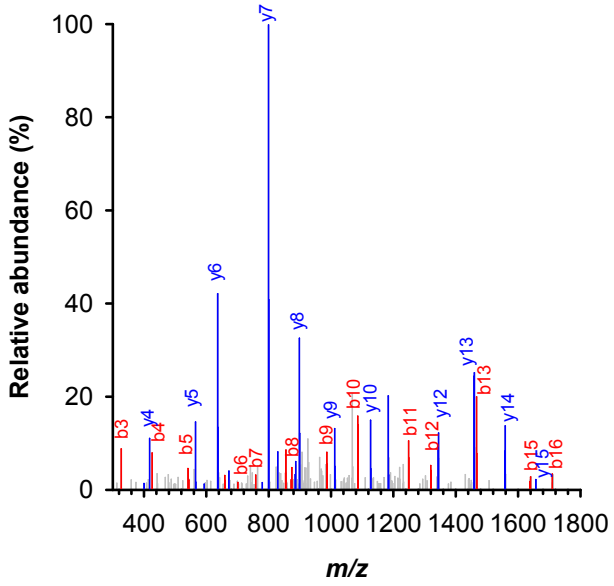

Assigned *b*- and *y*-ions

#	b+	b++	Seq.	y+	y++	#
1			L	1883.9	942.45	17
2	228.13		N	1770.81	885.91	16
3	327.2	164.11	V	1656.77	828.89	15
4	426.27	213.64	V	1557.7	779.35	14
5	541.3	271.15	D	1458.63	729.82	13
6	701.33	351.17	C#	1343.6	672.31	12
7	758.35	379.68	G	1183.57	592.29	11
8	873.38	437.19	D	1126.55	563.78	10
9	986.46	493.73	L	1011.53	506.27	9
10	1085.53	543.27	V	898.44	449.72	8
11	1248.59	624.8	Y	799.37	400.19	7
12	1319.63	660.32	A	636.31	318.66	6
13	1466.7	733.85	F	565.27	283.14	5
14	1523.72	762.36	G	418.2	209.61	4
15	1638.75	819.88	D	361.18	181.09	3
16	1709.78	855.4	A	246.16		2
17			R	175.12		1

Sequest results: *z*= +2, *m/z* 942.72 (mass error: -361.49 ppm), Xcorr = 5.49, SpScore = 1657.42

FIG S6(E) Assignment of the tandem mass spectrum to the predicted *b*- and *y*-ions of agmatinase (SpeB) 83LNVVDC#GDLVYAFGDAR99, which forms an intermolecular disulfide bond at Cys167.

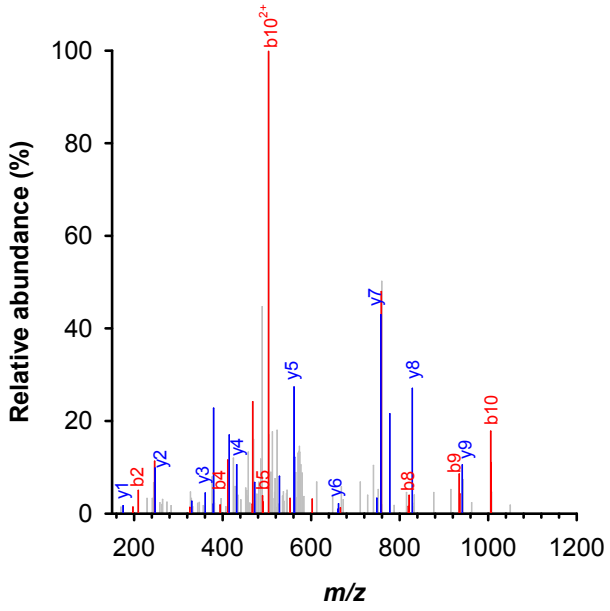

Assigned *b*- and *y*-ions

#	b+	b++	Seq.	y+	y++	#
1			A	1761.91	881.46	17
2	209.1		H	1690.87	845.94	16
3	266.13		G	1553.81	777.41	15
4	394.22	197.61	K	1496.79	748.9	14
5	491.27	246.14	P	1368.69	684.85	13
6	651.3	326.16	C#	1271.64	636.32	12
7	708.33	354.67	G	1111.61	556.31	11
8	821.41	411.21	I	1054.59	527.8	10
9	934.49	467.75	L	941.5	471.26	9
10	1005.53	503.27	A	828.42	414.71	8
11	1102.58	551.8	P	757.38	379.2	7
12	1201.65	601.33	V	660.33	330.67	6
13	1330.69	665.85	E	561.26	281.13	5
14	1401.73	701.37	A	432.22	216.61	4
15	1516.76	758.88	D	361.18	181.09	3
16	1587.8	794.4	A	246.16		2
17			R	175.12		1

Sequest results: *z*= +3, *m/z* = 588.54 (mass error: +325.79 ppm), Xcorr = 3.67, SpScore = 772.98

FIG S6(F) Assignment of the tandem mass spectrum to the predicted *b*- and *y*-ions of α-dehydro-β-deoxy-D-glucarate aldolase ^{208}AHGKPC#GILAPVEADAR^{224}, which forms an intermolecular disulfide bond at Cys213.

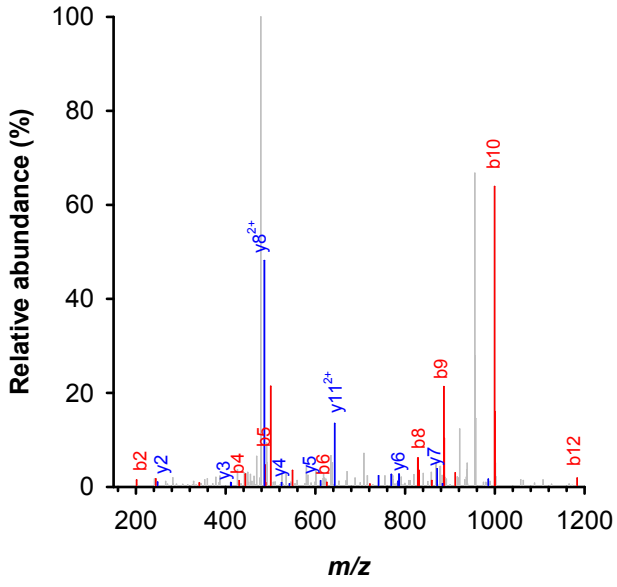

Assigned *b*- and *y*-ions

#	b+	b++	Seq.	y+	y++	#
1			I	1967.94	984.47	18
2	201.12		S	1854.85	927.93	17
3	300.19	150.6	V	1767.82	884.41	16
4	431.23	216.12	M	1668.75	834.88	15
5	488.25	244.63	G	1537.71	769.36	14
6	625.31	313.16	H	1480.69	740.85	13
7	682.33	341.67	G	1343.63	672.32	12
8	829.37	415.19	M*	1286.61	643.81	11
9	886.39	443.7	G	1139.58	570.29	10
10	999.48	500.24	I	1082.55	541.78	9
11	1096.53	548.77	P	969.47	485.24	8
12	1183.56	592.28	S	872.42	436.71	7
13	1357.61	679.31	C#	785.39	393.2	6
14	1444.64	722.82	S	611.34	306.17	5
15	1557.72	779.37	I	524.31	262.66	4
16	1720.79	860.9	Y	411.22	206.12	3
17	1821.83	911.42	T	248.16		2
18			K	147.11		1

Sequest results: oxidation of M65, *z*= +3, *m/z* 652.34 (mass error: -161.73 ppm), Xcorr = 2.88, SpScore = 700.74

FIG S6(G) Assignment of the tandem mass spectrum to the predicted *b*- and *y*-ions of purine nucleoside phosphorylase (DeoD) ^{58}ISVMGHGM*GIPSC#SIYTK^{75}, which forms an intermolecular disulfide bond at Cys70.

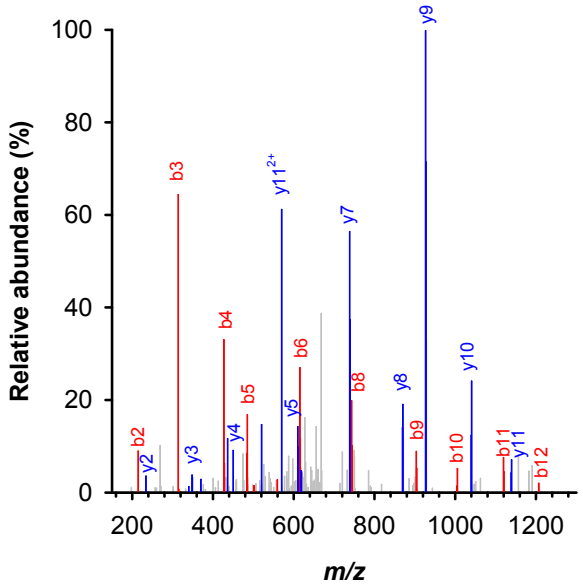

Assigned *b*- and *y*-ions

#	b+	b++	Seq.	y+	y++	#
1			D	1352.62	676.81	13
2	**215.1**		V	1237.59	**619.3**	12
3	**314.17**	157.59	V	**1138.52**	**569.76**	11
4	**427.26**	**214.13**	I	**1039.45**	**520.23**	10
5	**484.28**	242.64	G	**926.37**	463.69	9
6	**615.32**	308.16	M	**869.35**	**435.18**	8
7	672.34	336.67	G	**738.31**	**369.66**	7
8	**743.38**	372.19	A	681.29	**341.15**	6
9	**903.41**	452.21	C#	**610.25**	305.63	5
10	**1004.45**	**502.73**	T	**450.22**	225.61	4
11	**1119.48**	**560.24**	D	**349.17**	175.09	3
12	**1206.51**	603.76	S	**234.14**		2
13			K	147.11		1

Sequest results: *z*= +2, *m/z* = 677.58 (mass error: +431.88 ppm), Xcorr = 3.82, SpScore = 1153.89

FIG S6(H) Assignment of the tandem mass spectrum to the predicted *b*- and *y*-ions of purine nucleoside phosphorylase (DeoD) ^{103}DVVIGMGAC#TDSK^{115}, which forms an intermolecular disulfide bond at Cys111.

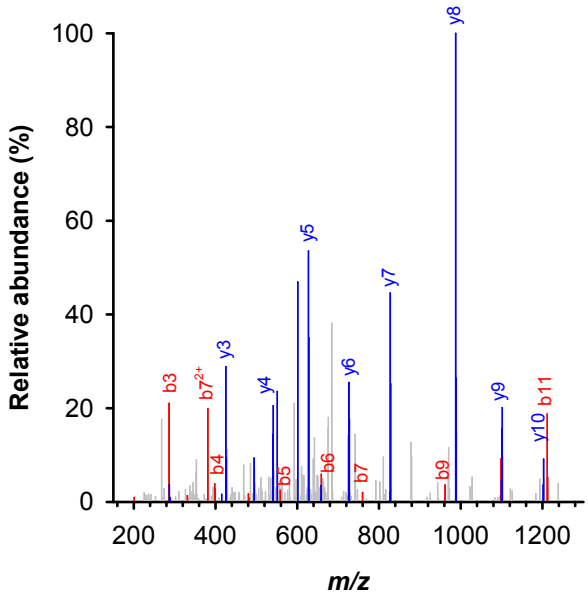

Assigned *b*- and *y*-ions

#	b+	b++	Seq.	y+	y++	#
1			A	1385.72	693.36	12
2	185.13		L	1314.68	**657.85**	11
3	**286.18**		T	**1201.6**	**601.3**	10
4	**399.26**	**200.13**	I	**1100.55**	**550.78**	9
5	**559.29**	280.15	C#	**987.47**	**494.24**	8
6	**660.34**	**330.67**	T	**827.44**	**414.22**	7
7	**759.41**	**380.21**	V	**726.39**	363.7	6
8	846.44	423.72	S	**627.32**	314.16	5
9	**961.47**	**481.24**	D	**540.29**	270.65	4
10	**1098.53**	549.77	H	**425.26**	213.13	3
11	**1211.61**	606.31	I	**288.2**		2
12			R	175.12		1

Sequest results: *z*= +2, *m/z* 693.68 (mass error: -188.23 ppm), Xcorr = 2.97, SpScore = 950.20

FIG S6(I) Assignment of the tandem mass spectrum to the predicted *b*- and *y*-ions of purine nucleoside phosphorylase (DeoD) ^{197}ALTIC#TVSDHIR^{208}, which forms an intermolecular disulfide bond at Cys201.

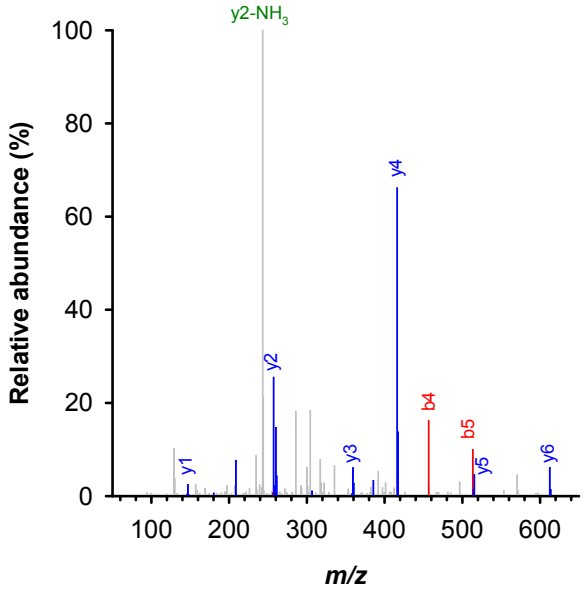

Assigned *b*- and *y*-ions

#	b+	b++	Seq.	y+	y++	#
1			C#	871.52	436.26	8
2	260.12		R	768.51	384.76	7
3	357.17	179.09	P	612.41	306.71	6
4	456.24	228.62	V	515.35	258.18	5
5	513.26	257.13	G	416.29	208.65	4
6	612.33	306.67	V	359.26	180.14	3
7	725.41	363.21	L	260.2		2
8			K	147.11		1

Sequest results: *z*= +3, *m/z* = 310.40 (mass error: -4.16 ppm), Xcorr = 2.62, SpScore = 916.78

FIG S6(J) Assignment of the tandem mass spectrum to the predicted *b*- and *y*-ions of inorganic pyrophosphatase (Ppa) ^{88}C#RPVGVLK^{95}, which forms an intermolecular disulfide bond at Cys88.

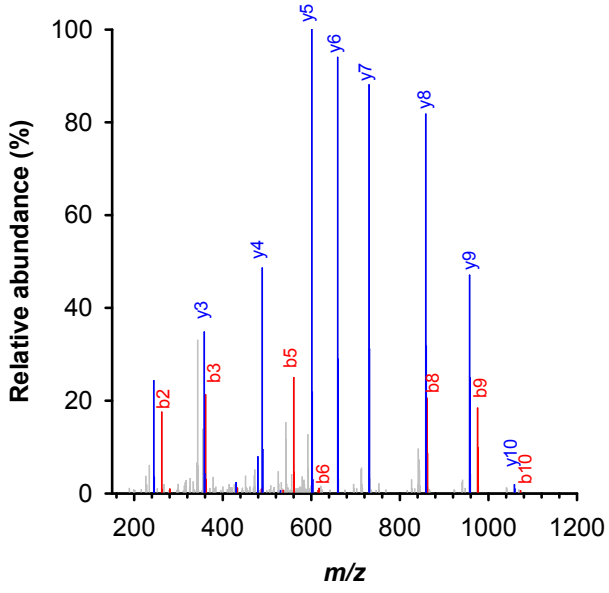

Assigned *b*- and *y*-ions

#	b+	b++	Seq.	y+	y++	#
1			C#	1218.6	609.8	11
2	262.09		T	1058.57	529.79	10
3	361.15	181.08	V	957.52	479.26	9
4	489.21	245.11	Q	858.45	429.73	8
5	560.25	280.63	A	730.39	365.7	7
6	617.27	309.14	G	659.35	330.18	6
7	730.36	365.68	L	602.33	301.67	5
8	861.4	431.2	M	489.25	245.13	4
9	975.44	488.22	N	358.21	179.61	3
10	1072.49	536.75	P	244.17		2
11			K	147.11		1

Sequest results: *z*= +2, *m/z* 610.30 (mass error: +92.58 ppm), Xcorr = 3.57, SpScore = 1754.18

FIG S6(K) Assignment of the tandem mass spectrum to the predicted *b*- and *y*-ions of translation initiation inhibitor (YoaB) ^{93}C#TVQAGLMNPK^{103}, which forms an intermolecular disulfide bond at Cys93.

TABLE S1 Bacterial strains and plasmids used in this study

Strains or plasmids	Relevant characteristics	References
Strains of *Salmonella enterica* Serovar Typhimurium		
ATCC14028S	wild-type	Fields et al., 1986
ΔmdsABC	*ΔmdsABC*::Cm^R	This study
ΔacrABΔtolC	*ΔacrABΔtolC*::Tn^R	This study
ΔacrABΔtolCΔmdsABC	*ΔacrABΔtolC*::Tn^R *ΔmdsABC*::Cm^R	This study
Plasmids		
pKD3	$rep_{R6K\gamma[p]}$ Ap^R FRT Cm^R FRT	Datsenko and Wanner, 2000
pKAN6B	p15A *ori*, Km^R	Yeom and Lee, 2006
pMdsAB	*mdsAB* genes cloned into pKAN6B, Km^R	This study
pMdsABC	*mdsABC* genes cloned into pKAN6B, Km^R	This study

TABLE S2 Primers used in this study.

Experiments	Primer name	Oligonucleotide sequence (5' to 3')
Gene deletion	AcrA-H1P1	TTGAAATCGGACACTCGAGGTTTACATATGAACAAAAACGTGTAGGCTGGAGCTGCTTC
	AcrB-H2P2	CGGCTAAAGCGGCGGCGTACCACCACGAAGAAGACCGGTATATGAATATCCTCCTTA
	TolC-H1P1	TCAGCGCTAAATACTGCTTCACAACAAGGAATGCAAATGAGCACCTGAAGTCAGCCCCA
	TolC-H2P2	TTGCCGTTATTGCTGTTGGCGCGAGCGGCGGTCGGCTGTGAGTGGTGAATCCGTTAGCG
	MdsA-H1P1	TGCGGAATGGCCGACACGCTGCGGTAAAGAGGGAAACGACGTGTAGGCTGGAGCTGCTTC
	MdsC-H2P2	TAGCGCGCGCGCCGCACTGGCGACGCGGGCGCTATTTGGGCATATGAATATCCTCCTTAG
Gene cloning	MdsA-F_*Nde*I	CGCATATGCGTAGAACATTCAAAATTATGTTGATAGC
	MdsB-R_*Xba*I	TATCTAGATTATGCTTGCTGATCATGCG
	MdsB-F_*Sse*8387I	GGCCTGCAGGGTGAGTTTTATCGTCAG
	MdsB-R_*Sse*8387I	AACTCACCCTGCAGGCCCGCCAGGAATG
	MdsC-R_His_XbaI	CGTCTAGACTAATGATGATGATGATGATGACCTTGCTTTTTCTCACTGTATTCCCGCCA
RT-PCR	*mdsA*-F	CTGTTTGCCCGAATCAGTTT
	mdsA-R	AGTCAATGTCGCGGTCTGTT
	mdsB-F	CGAATACCGGATTGCCTATG
	mdsB-R	GAGATATGCCGTTCCACGTT
	mdsC-F	CTTCCACGATCCGCTTCTAC
	mdsC-R	GCTAATGCCTGGTCGCTAAG
	cdsA-F	GTCAACCGCTGGTTGAGATG
	cdsA-R	ACCTTCGGCGCCAGCTTATG
	pssA-F	CATTGATGATAGCGTCCTGTACAGCG
	pssA-R	CCAGTACCGCTGGTAGATTGAAGTAAG
	tolC-F	GCCCGTGCGCAATATGATACCGTACTGG
	tolC-R	GCTGTATCAAGGTGGGATGGTTAACTCG
	16S rRNA-F	CTGACGCTCAGGTGCGAAAG

	16S rRNA-R	TCACAACACGAGCTGACGAC
	dnaK-F	CGTATGCCAATGGTGCAGAA
	dnaK-R	ACTGGTTGTCTTCCGCAGTA

TABLE S3 Fatty acid methyl ester profiles of wild-type (WT), *mdsABC* deletion (DT), and *mdsABC* expression mutant (MT) strains of *S.* Typhimurium 14028S.

Fatty acid components	WT	DT	MT	Sum in Features
13:0	0.64±0.02	0.51±0.07	1.73±0.21	
14:1 ω5c	2.90±0.07	2.45±0.20	4.38±0.30	
14:0	2.64±0.16	3.00±0.29	3.12±0.21	
15:0 anteiso			0.53±0.21	
14:0 2OH			1.29	
Sum in Feature 2	7.32±0.24	8.51±0.99	8.15±1.07	14:0 3OH/16:1 iso I
16:0 N alcohol	3.03±0.32	2.10±0.25	1.97	
16:1 ω11c	2.90±0.10		3.86±0.10	
16:1 ω5c		0.54		
16:1 ω7c alcohol			1.56±0.86	
Sum in Feature 3	0.95±0.02		1.29±0.10	16:1 ω6c/16:1 ω7c
16:0	36.2±1.49	38.8±4.24	40.6±0.36**	
16:0 iso 3OH	3.09±0.25	4.40±0.21	3.55±0.01	
17:1 iso ω5c		11.6±1.19		
17:1 anteiso A	11.9±1.42	2.38±0.38		
17:1 anteiso ω9c			3.55±0.11	
17:0 cyclo	2.45±0.14	9.81	7.53	
17:0	10.3±0.61			
18:3 ω6c (6,9,12)	3.65±0.22	2.99±0.28	3.55±0.20	
18:0	5.28±0.20	6.03±0.25	5.02±0.22	
17:0 iso 3OH	1.28±0.90	1.37±0.52	1.90±0.61	
19:1 iso I			4.34	
19:0 iso	2.49±0.13	2.70±0.54	0.80±0.35	
19:0 cyclo ω8c	3.02±0.17	2.90±0.29	1.29±0.08	

A statistically significant difference in the level of palmitate ($C_{16:0}$) methyl ester (**$P < 0.01$) analyzed by two-tailed *t*-test between the results obtained from three independent cultures of MT and WT strains in mMOPS media containing 0.1% glucose, 0.1% arabinose, and 100 μg mL^{-1} kanamycin.

TABLE S4 Mass spectrometry data of disulfide-forming proteins identified by diagonal gel analyses of cytosolic and membrane fractions obtained from *Salmonella enterica* serovar Typhimurium 14028S.

Spot#	GI number	Gene	Protein description	Score	Coverage	# Unique peptides	#PSM	MW[kDa]	calc. pI	Reactive cysteine
			Peptide sequence	SpScore	XCorr	#PSM	Charge	MH+ [Da]	ΔM [ppm]	m/z [Da]
C1	378450316	adhE	acetaldehyde-CoA/alcohol dehydrogenase	175.13	27.02	19	56	96.15	6.65	C246
			AADIVLQAAIAAGAPK	3303.03	5.42	5	2	1480.27	-324.81	740.64
			mAVAESGmGIVEDK	1995.74	3.95	4	2	1470.09	280.13	735.55
			YAEIADHLGLSAPGDR	1846.01	3.90	2	3	1685.36	-281.93	562.46
			MAVAESGmGIVEDK	1811.94	3.80	2	2	1452.47	-835.75	726.74
			GSLPIALDEVITDGHK	779.16	3.70	1	2	1665.34	-329.78	833.17
			AAALAAADAR	1394.47	3.69	8	2	900.76	-276.74	450.88
			EAGVQEADFLAHVDK	756.41	3.63	1	2	1629.34	-263.55	815.17
			FLFNNGYADQITSVLK	1047.51	3.62	2	2	1831.58	272.46	916.29
			NHFASEYIYNAYKDEK	970.73	3.60	1	3	1993.07	-36.51	665.03
			NGALNAAIVGQPAYK	1797.52	3.57	5	2	1489.17	983.98	745.09
			AVASVLmSK	857.34	3.24	2	2	921.99	-158.78	461.50
			AKDFEEAVEK	1109.82	3.19	4	3	1166.25	-16.69	389.42
			YNANDNPTK	867.23	3.15	4	2	1036.96	-109.32	518.98
			EYASFTQEQVDK	975.61	3.09	2	2	1445.06	-319.88	723.04
			FASHGGYmLQGQELK	447.43	2.99	1	3	1682.58	-191.32	561.53
			IAELAGFSVPETTK	662.44	2.97	3	2	1463.30	-254.29	732.15
			NAIIFSPHPR	1168.26	2.91	4	2	1152.35	8.67	576.68
			QILLDTYYGR	426.33	2.84	1	2	1243.38	769.78	622.19
			AVASVLMSK	623.89	2.63	1	2	905.98	-166.69	453.50
			DFTEGEVAAK	565.90	2.54	1	2	1066.85	-269.61	533.93
			YPLISELK	804.04	2.50	2	2	962.40	-797.28	481.70
M1	378451702	cysJ	sulfite reductase subunit alpha	75.58	17.53	10	23	66.44	5.03	C162, C552
			AGGASSFLADRVEEEGEVR	1603.29	5.09	3	3	1979.80	-148.99	660.61
			VTLISASQTGNAR	1474.48	3.65	4	2	1318.13	-260.78	659.57
			HIEIDLGDSGLR	1556.58	3.60	2	2	1324.46	-761.59	662.73
			VDADVEYQAAASEWR	2062.93	3.52	1	2	1709.95	-497.45	855.48
			GDEPVTVDGK	1002.81	3.34	4	2	1016.79	-284.59	508.90

			DAPLIATLSVNQK	894.71	3.23	1	2	1370.17	-306.72	685.59
			AGGASSFLADR	1418.53	3.18	2	2	1052.13	-2.13	526.57
			SGAVAVTPVPER	421.11	3.12	4	2	1182.90	-376.95	591.96
			VEEEGEVR	656.32	2.98	1	2	946.87	-131.99	473.94
			SESLLPLVGDK	1060.27	2.85	1	2	1158.04	-257.66	579.52
M2	378449732	oppA	ABC transporter periplasmic binding protein	58.16	19.12	8	17	59.99	7.15	C297-C443
			DANDYPVGNDVTADVAIR	862.84	5.10	3	2	1906.57	291.52	953.79
			FSDGSPLTAEDVVFTYNK	1092.29	4.51	4	3	1991.04	-61.95	664.35
			IAPSmAVAPQQDNLK	608.67	3.60	2	2	1599.30	-344.18	800.15
			LVFVFLDEDNAYAAAR	1205.06	3.28	1	2	1815.74	387.75	908.37
			LTLWYASGDSTR	1049.38	3.26	1	2	1370.21	-219.29	685.61
			IAPSMAVAPQQDNLK	907.18	3.25	1	2	1584.08	145.48	792.54
			IDmGNFSHAR	759.35	3.02	1	2	1165.22	799.49	583.11
			AINYAINR	288.97	2.32	1	1	934.47	-639.77	934.47
			DLAEAVR	326.85	2.16	3	1	773.45	-534.44	773.45
M3	378452157	codA	cytosine deaminase	32.71	13.15	4	9	47.60	6.40	[c215]
			LGADVIGAIPHFEFTR	1401.33	4.07	4	2	1743.55	-258.38	872.28
			THVDVSDPTLTALK	1121.49	3.71	2	2	1498.33	425.72	749.67
			FVETVAALAHR	1069.26	3.49	2	2	1214.08	-274.13	607.54
			LIDVHcDEIDDEQSR	1029.82	3.48	1	2	1844.44	-278.26	922.72
M4	378450822	fba	fructose-bisphosphate aldolase	83.30	24.57	7	23	38.06	6.87	C112
			AGLINSGGADGGDTDLGDAVR	1959.55	5.60	3	2	1931.54	-240.97	966.28
			LINAVQDVYLDSK	1734.97	4.42	3	2	1478.48	-138.71	739.74
			LTSDNPIDLVR	1368.38	3.70	6	2	1243.02	-305.08	622.02
			RQIEEISAAFER	918.06	3.58	1	2	1448.34	-874.36	724.67
			AGGmGLILGR	1442.83	3.48	2	2	961.10	-75.33	481.05
			DADSLLQHR	1248.29	3.36	5	2	1054.31	-780.15	527.66
			AVNFGYTDDR	1108.35	3.29	1	2	1158.18	-29.11	579.59
			AGGMGLILGR	1038.68	2.96	2	2	943.95	-1301.60	472.48
M5	378453486	iaaA	isoaspartyl dipeptidase	15.74	11.28	3	5	40.30	5.96	C229
			SAAPSGNQLASmAAESR	560.19	4.03	2	2	1664.20	-354.39	832.61
			LTEAGITTVVGLLGTDSVSR	637.37	3.43	2	2	1990.38	58.96	995.69
			DVALIDR	387.07	1.92	1	1	801.59	-411.50	801.59
M6	378451259	bamB	outer membrane protein subunit	15.51	12.76	3	4	41.92	4.86	C20

			VDSSGFLTEPTVADGK	1209.26	4.37	2	2	1623.33	-261.30	812.17
			GESAPATAFGAAIVGGDNGR	1559.00	4.22	1	2	1819.22	155.59	910.12
			ELGSVNDFIVDGDR	994.94	3.38	1	2	1536.32	-208.91	768.66
M7	378450994	glpQ	glycerophosphodiester phosphodiesterase	126.36	39.33	14	41	40.40	6.05	[c206]
			AGVDGLFTDFPDK	1718.95	4.52	8	2	1382.28	-169.35	691.64
			DDHLVVLHDHYLDR	1497.59	4.03	5	3	1747.69	-124.78	583.24
			LTGMVQDAHQNK	1239.44	3.78	3	2	1342.06	-343.45	671.53
			LTGmVQDAHQNK	778.12	3.64	5	2	1358.31	-151.07	679.66
			QDNVYLQcFDVAELK	1174.74	3.21	1	2	1842.94	-68.95	921.97
			GASGYLPEHTLPAK	701.01	2.97	4	2	1441.39	-164.07	721.20
			YYAIDFTLDEIK	788.96	2.90	1	2	1491.25	-289.04	746.13
			IKNELEPK	1233.20	2.84	5	3	971.24	98.08	324.42
			VTDVADRFPDR	502.41	2.80	1	3	1291.88	369.02	431.30
			FTEGFDIENGK	1130.86	2.80	2	2	1258.07	575.16	629.54
			TLEVLKK	536.04	2.67	1	2	830.97	-88.65	415.99
			FTEGFDIENGKK	1150.94	2.62	1	2	1386.29	555.20	693.65
			MVVHPYTVR	546.27	2.59	1	2	1101.98	-338.59	551.49
			YGYTGK	396.56	2.08	2	1	688.45	-452.84	688.45
			AVMFLQK	660.79	1.94	1	1	836.50	-691.93	836.50
M8	378451892	ansB	L-asparaginase II	159.50	37.93	10	46	36.90	6.25	C99-C127
			VGIVYNYANASDLPAK	2042.38	4.98	6	2.00	1695.52	-234.94	848.26
			GVLVVmNDTVMDGR	1821.96	4.51	7	2.00	1523.39	393.49	762.20
			VPTGATTQDAEVDDAK	1281.33	4.36	5	2.00	1618.47	-136.10	809.74
			GVLVVmNDTVmDGR	1717.43	4.28	6	2.00	1538.13	-425.90	769.57
			VLLQLALTQTK	1996.12	4.14	3	2.00	1228.16	-289.89	614.59
			YGFVASGTLNPQK	1761.46	4.12	6	2.00	1382.14	-304.74	691.57
			VGVENLVDAVPQLK	1287.96	4.08	2	2.00	1481.45	-190.69	741.23
			GVLVVMNDTVMDGR	751.51	3.39	1	2.00	1507.44	433.05	754.22
			AVNYGPLGYIHNGK	1115.02	3.00	2	2.00	1504.43	486.57	752.72
			TVFDTLATAAHNGTVVVR	763.03	2.97	2	2.00	1873.66	285.37	937.33
			TNTTDVATFK	507.19	2.69	1	2.00	1097.89	-278.76	549.45
			DIAVVK	597.29	2.00	5	1.00	644.47	-488.65	644.47
M9	378448281	talB	transaldolase B	517.55	47.95	17	172	35.15	5.22	[c167], [c239]

			QFTTVVADTGDIAAmK	1588.68	4.84	10	2	1684.47	-258.64	842.74
			LYNDAGISNDR	1863.40	4.28	20	2	1238.25	-39.43	619.63
			NVGEILELAGcDR	1551.42	3.89	6	2	1446.46	-111.11	723.74
			QFTTVVADTGDIAAMK	1439.22	3.76	7	2	1668.37	-321.20	834.69
			LIDDAVAWAK	795.94	3.75	5	2	1102.09	-167.14	551.55
			KLIDDAVAWAK	2029.07	3.72	4	2	1230.23	-180.14	615.62
			ELAESEGAIER	1277.35	3.62	20	2	1204.18	-84.40	602.59
			LSYDTEASIAK	1087.50	3.57	19	2	1198.19	-104.75	599.60
			AcAEAGVYLISPFVGR	1412.76	3.55	7	3	1710.65	-201.88	570.89
			AQQVVDATDK	865.02	3.20	42	2	1074.98	-169.30	537.99
			QHGYETVVMGASFR	808.24	3.06	3	3	1582.87	56.39	528.30
			LSYDTEASIAKAK	1481.48	2.99	2	2	1396.19	-984.86	698.60
			QHGYETVVmGASFR	1096.00	2.94	7	3	1598.54	-151.27	533.52
			LASTWQGIR	1027.19	2.93	3	2	1032.00	-178.63	516.51
			KLIDDAVAwAK	1017.62	2.87	1	2	1245.74	-573.99	623.37
			NVGEILELAGCDR	1541.44	2.82	1	2	1389.76	133.21	695.38
			LIDDAVAwAK	753.01	2.74	2	2	1118.14	-119.99	559.57
			KFAVDQEK	832.95	2.57	3	2	964.92	-180.53	482.96
			IIKLYNDAGISNDR	696.51	2.45	1	2	1591.41	-871.96	796.21
			KLSFSGEVK	386.45	1.94	4	1	994.70	-471.36	994.70
			ISTEVDAR	154.67	1.93	1	1	890.48	-544.29	890.48
			FAVDQEK	503.04	1.89	4	1	836.42	-598.36	836.42
M10	378451863	speB	agmatinase	81.16	22.88	5	22	33.58	5.59	[c88]
			LNVVDcGDLVYAFGDAR	1657.42	5.49	7	2	1884.43	-361.49	942.72
			mLSFGGDHFVTLPLLR	964.48	4.87	4	2	1819.43	-405.02	910.22
			GVDDILAQVK	1387.00	3.79	8	2	1057.92	-281.25	529.47
			EGLIDPHHSVQIGIR	668.45	3.34	1	3	1671.81	-55.66	557.94
			MLSFGGDHFVTLPLLR	529.60	2.82	1	3	1802.77	-774.38	601.60
			QVSTNLAWEHHR	371.12	2.81	1	2	1478.35	-177.72	739.68
M11	378452068		α-dehydro-β-deoxy-D-glucarate aldolase	6.69	10.55	2	2	27.30	6.29	[c213]
			AHGKPcGILAPVEADAR	772.98	3.67	1	3	1763.61	325.79	588.54
			VPTNEPVIIK	488.23	3.02	1	2	1110.13	-187.66	555.57
M12	378453554	deoD	purine nucleoside phosphorylase	183.97	39.33	10	54	25.96	5.86	[c70], [c111], [c201]
			DHDFAAIADFDMVR	2476.56	5.52	3	2	1624.27	296.88	812.64

			FKDHDFAAIADFDmVR	1613.00	4.49	5	3	1915.01	-69.45	639.01
			DHDFAAIADFDmVR	2427.61	4.46	6	2	1638.58	-738.63	819.79
			FKDHDFAAIADFDMVR	1411.23	4.40	3	3	1898.93	-108.89	633.65
			IALESVLLGDKE	2461.87	4.24	8	2	1287.30	-151.66	644.15
			LRDVVIGMGAcTDSK	2004.17	4.13	3	3	1622.17	-457.40	541.39
			DVVIGMGAcTDSK	1153.89	3.82	3	2	1354.15	431.88	677.58
			LRDVVIGmGAcTDSK	1546.66	3.74	3	3	1638.18	-445.00	546.73
			IALESVLLGDK	1314.29	3.64	2	2	1158.02	-308.05	579.52
			HIAETFLENVR	628.39	3.62	5	2	1329.25	-187.92	665.13
			DVVIGmGAcTDSK	863.62	3.59	4	2	1370.11	404.30	685.56
			ALTIcTVSDHIR	950.20	2.97	2	2	1386.36	-188.23	693.68
			ISVMGHGmGIPScSIYTK	700.74	2.88	1	3	1955.02	-161.73	652.34
			GmLGFTGTYK	868.84	2.86	4	2	1090.79	-446.47	545.90
			GMLGFTGTYK	516.43	2.85	2	2	1075.86	544.69	538.43
M13	378448475	yadF	carbonic anhydrase	113.24	26.36	6	38	24.81	6.04	C42, C101
			mKDIDTLISNNALWSK	1895.57	3.99	1	3	1867.11	512.36	623.04
			mLVEEDPGFFEK	1183.22	3.83	8	2	1458.00	243.22	729.50
			LTGLEPGELFVHR	875.22	3.60	4	2	1468.15	-370.78	734.58
			DIDTLISNNALWSK	1280.97	3.60	1	2	1591.62	533.11	796.32
			MLVEEDPGFFEK	1315.65	3.53	7	2	1441.07	-400.24	721.04
			DLDVTATNR	1103.11	3.37	15	2	1004.97	-100.61	502.99
			GISALSLK	664.36	2.05	2	1	788.58	-483.85	788.58
M14	378449942	sodB	Fe-superoxide dismutase	1275.61	33.16	6	321	21.32	5.95	C80
			LADAIAASFGSFAEFK	2569.42	6.24	247	2	1646.55	420.58	823.78
			HHQTYVTNLNNLIK	2712.20	4.78	33	3	1695.17	-442.68	565.73
			NFGSGWTWLVK	658.88	3.15	8	2	1295.15	-262.73	648.08
			AQFTDAAIK	533.04	2.37	21	1	964.62	-492.21	964.62
			GTAFEGKSLEEIVR	294.51	2.30	1	2	1535.43	-846.81	768.22
			SLEEIVR	383.04	2.04	11	1	845.54	-516.69	845.54
M15	378453372	ppa	inorganic pyrophosphatase	106.03	49.43	10	38	19.66	5.17	[c88]
			YEVDKESGALFVDR	2335.63	4.84	4	2	1628.37	-251.54	814.69
			EYDHIKDVNDLPELLK	413.68	3.58	4	3	1943.04	442.01	648.35
			AEIVASFER	1126.17	3.20	6	2	1021.93	-212.56	511.47
			VDGWDNAEAAK	1181.83	3.11	4	2	1176.00	-198.31	588.50

			ESGALFVDR	685.57	3.05	5	2	993.89	-204.90	497.45
			VDGwDNAEAAK	1421.94	3.01	1	2	1191.92	-256.30	596.46
			cRPVGVLKMTDESGEDAK	506.29	2.95	1	2	1993.06	-104.46	997.04
			DVNDLPELLK	679.81	2.93	4	2	1156.17	-133.35	578.59
			cRPVGVLK	916.78	2.62	4	3	929.17	-4.16	310.40
			AQITHFFEHYK	247.91	2.59	2	3	1422.11	355.55	474.71
			LVAVPHTK	672.73	2.57	3	2	864.79	-320.23	432.90
M16	378449942	sodB	superoxide dismutase	206.29	8.29	1	50	21.32	5.95	C42, C101
			LADAIAASFGSFAEFK	1946.58	5.43	50	2	1646.26	247.89	823.63
M17	378453420	yjgF	putative translation initiation inhibitor	81.02	34.38	5	25	13.57	5.24	C107
			TGAVAEDVSAQAR	1475.25	4.13	14	2	1275.15	-162.26	638.08
			IEIEAIAVR	1060.29	3.48	5	2	1014.60	387.52	507.81
			QSLENVKAIVEAAGLK	593.73	2.67	1	2	1669.84	-666.38	835.42
			AIVEAAGLK	848.47	2.34	4	1	871.57	-555.47	871.57
			TTVFVK	549.51	1.95	1	1	694.49	-514.24	694.49
M18	378450404	yoaB	putative translation initiation inhibitor	127.20	43.86	5	43	12.58	5.01	[c93]
			AWDAWVVAGHAPVR	1813.58	4.49	6	2	1536.28	344.97	768.64
			ILDATIFLSDK	1117.93	4.00	7	2	1236.23	-176.60	618.62
			AWDAwVVAGHAPVR	1835.62	3.62	1	2	1551.36	-252.32	776.18
			cTVQAGLMNPK	1754.18	3.57	2	2	1219.59	92.58	610.30
			cTVQAGLmNPK	987.95	3.51	11	2	1235.75	227.18	618.38
			AwDAwVVAGHAPVR	766.89	2.74	1	2	1567.05	-446.49	784.03
			ADFAAMNK	614.06	2.45	12	1	867.43	-657.57	867.43
			YKVEIK	507.41	1.98	3	1	779.55	-524.35	779.55
M19	378452286	slyD	peptidyl-prolyl cis-trans isomerase	401.36	18.88	4	134	20.77	4.93	C167, C168, C184, C185, C193
			DVFMGVDELQVGMR	1892.09	4.32	1	2	1596.29	-367.47	798.65
			DVFmGVDELQVGMR	1956.93	4.23	9	2	1612.43	-276.66	806.72
			DVFmGVDELQVGmR	2181.88	4.13	38	2	1629.19	195.60	815.10
			FNVEVVAIR	1564.78	3.76	42	2	1046.47	-737.43	523.74
			DLVVSLAYQVR	1255.34	3.65	42	2	1263.88	312.81	632.44
			VPKDVFmGVDELQVGmR	524.67	3.34	2	2	1952.51	-403.11	976.76

Footnotes.

Protein spots excised from diagonal gels are same as shown in Fig. 5A in the main text.

Gene symbols were obtained from identical genes in the GenBank and UniProtKB/Swiss-Prot databases of S. enteria, except for α-dehydro-β-deoxy-D-glucarate aldolase (PRK10558).

Protein spots excised from diagonal gels were differently modified by N-ethylmaleimide and iodoacetamide, respectively, before and after the reduction of disulfide bond with dithioreitol in order to identify free thiol and disulfide cysteine residues.

Proteins were identified by using the Sequest search engine of Thermo Proteome Discoverer version 1.3 against the database of S. Typhimurium 14028S (downloaded from GenBank) and the common Repository of Adventitious Proteins (downloaded from URL ftp://ftp.thegpm.org/fasta/cRAP) with the following options: average mass (*m/z*); 1 miscleavage site of trypsin disgestion; precursor mass tolerance, 1.5 Da; fragment mass error, 0.8 Da; variable modifications for *N*-ethylmaleimide of free cysteine (designated as C#), carbamidomethylation of cysteine (lowercase 'c'), oxidation of methionine (lowercase 'm') and tryptophan (lowercase 'w').

Peptide spectrum matches (PSMs) were filtered out with the probability of >0.99 and the target-decoy false-discovery rate (FDR) of <0.01.

Disulfide-formed cysteines modified by iodoacetamide (lowercase 'c') are shown in the brackets with the positions in the protein sequence, and tandem mass spectra of identified peptides are shown in Fig. S5.

The predicted positions of reactive cysteine (uppercase 'C') and intramolecular disulfide (hyphen between 'C-C') analyzed from the UniProtKB/Swiss-Prot database are included in the list of Reactive cysteines.

Supplementary References

Datsenko KA, Wanner BL. 2000. One-step inactivation of chromosomal genes in *Escherichia coli* K-12 using PCR products. Proc. Natl. Acad. Sci. USA 97:6640-6645.

Fields PI, Swanson RV, Haidaris CG, Heffron F. 1986. Mutants of *Salmonella typhimurium* that cannot survive within the macrophage are avirulent. Proc. Natl. Acad. Sci. USA 83:5189-5193.

Song S, Hwang S, Lee S, Ha NC, Lee K. 2014. Interaction mediated by the putative tip regions of MdsA and MdsC in the formation of *Salmonella*-specific tripartite efflux pump. PLoS ONE. 9:e100881.

Yeom JH, Lee K. 2006. RraA rescues *Escherichia coli* cells over-producing RNase E from growth arrest by modulating the ribonucleolytic activity. Biochem. Biophys. Res. Commun. 345:1372-1376.